

Stretching a double-stranded DNA: Nature of the *B*-form to the *S*-form transition

Pik-Yin Lai^{a)}

Department of Physics and Center for Complex Systems, National Central University, Chung-li, Taiwan 320, Republic of China

Zi-cong Zhou

Department of Physics, Tamkang University, Tamsui, Taiwan 251, Republic of China

(Received 5 December 2002; accepted 25 March 2003)

The abrupt extension of the contour length and the self-unwinding of the double helix in the transition from the *B*-form to *S*-form of a double-stranded DNA under a stretching force is investigated in the framework of the model with basepair interactions and bending [Phys. Rev. Lett. **22**, 4560 (1999)]. In the region where thermal fluctuations can be neglected the classical mechanical approach is employed and equations governing the detail structure of the DNA are derived with some analytical results obtained. The transition from the *B*-form to *S*-form can be understood in terms of an effective potential with a barrier separating these two states and resulting in a first-order transition. The double helix of the DNA is almost fully unwound across the transition. Detail structural configurations, such as the loci of the two strands, relative extension, linear extension coefficient, and the threshold stretching force are calculated. The mean torque release as the dsDNA untwist across the transition is also estimated. These results are in agreement with various experimental data. © 2003 American Institute of Physics. [DOI: 10.1063/1.1574795]

I. INTRODUCTION

The DNA molecule is a double-stranded(ds) biopolymer with two complementary sugar-phosphate chains (*backbones*) twisted around each other to form a right-handed helix with one turn per 10.5 basepairs (bp).¹ Each chain is a linear polynucleotide consisting of four kind of bases: two purines (A, G) and two pyrimidines (C, T).^{1,2} The two chains are joined together by hydrogen bonds (*basepairs*) between pairs of nucleotides A–T and G–C. The distance between adjacent bases is about 0.34 nm. The novel elasticity of an individual double-stranded DNA (dsDNA) has recently attracted considerable interests both experimentally^{3–15} and theoretically.^{16–32} Three important deformations occurs for a dsDNA molecule: stretching or bending of the molecule or twisting of one nucleotide chain relative to its counterpart. All these deformations are of biological importance. For instance, during DNA replication, hydrogen bonds between the complementary DNA bases should be broken and the two nucleotide chains should be separated. This strand-separation process requires cooperative unwinding of the double-helix.² Another example is that in the DNA recombination reaction, RecA proteins polymerize along the DNA template and the DNA molecule is stretched to 1.5 times of its relaxed contour length.^{14,15}

Single molecule force experiments on dsDNA revealed that the elastic response of a dsDNA has clearly four regimes^{6,7,13} as depicted in Fig. 1. At first, it requires only a small force (< 10 pN) to remove thermal bending from the random coil and to extend to its native *B*-form conformation.

It follows a rather rigid regime up to a force of about 65 pN. With further increasing the external force, another narrow region appears and the dsDNA chain becomes highly extensible again up to a force of about 75 pN where a new conformation, the so-called *S*-form DNA, emerges. The contour length of *S*-DNA is about 1.7 times of the *B*-form. Beyond about 75 pN, a very large force is needed again for the further extension. It is believed that the change of the *B*-form to the *S*-form of the dsDNA is of biological importance before the double helix opens up in the transcription process to produce the messenger RNA and also during the duplication process. The increase of 1.7 times in the contour of the DNA from the *B*-form to *S*-form is quite universal for different types of DNA and hence we believe that the fundamental interactions among the basepairs should play an vital role in this elongation process. Thus an understanding of the fundamental mechanism of the change from the *B*-form to the *S*-form is of both physical and biological interest. Moreover, the applying of external torques result in some other novel behaviors.^{5–7,13} The linking number of DNA, i.e., the total topological turns one DNA strand winds around the other, can be fixed at a value larger (positive supercoiled) or smaller (negative supercoiled) than its *B*-form's value. Experiment observed that when the external force is smaller than a threshold value of about 0.3 pN, the elastic response of positively supercoiled DNA is similar to that of negatively supercoiled DNA. However, if the external force is increased to out of this threshold, negatively and positively supercoiled DNA molecules show very different behavior.

On the theoretical side, how to understand systematically and quantitatively all these mechanical properties of DNA based on the same unified framework is still a challenge in

^{a)}Electronic mail: pylai@phy.ncu.edu.tw

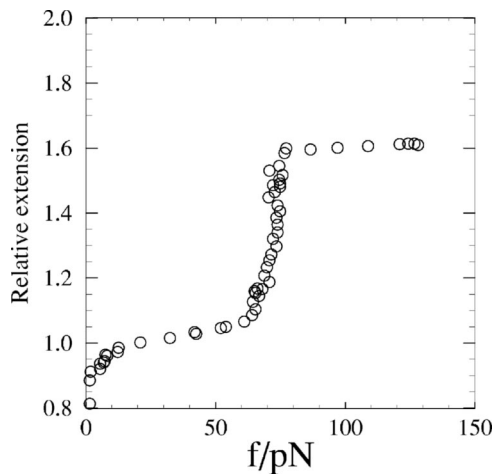


FIG. 1. Force experimental data of stretching a DNA in Ref. 6.

our time. Recently Zhou, Zhang, and Ou-Yang (ZZO) (Refs. 17, 18) proposed a new model based on bending and base-stacking interactions for the dsDNA. Using the Green function approach in polymer physics, they obtained numerical results for the elastic behavior of a dsDNA under external force and torque which agree very well with experimental data, except that the transition from the *B*-form to *S*-form is somewhat sharper than predicted. Only the ground state eigenvalue and eigenfunction were calculated numerically to obtain the average extension and probability distribution of the folding angles.^{17,18} On the other hand, the detail structural configurations of the dsDNA and especially the nature of the *B*-form to *S*-form transition are of fundamental and practical importance in the understanding of the elastic behavior of the dsDNA. Our recent work has shown that the ZZO model reduces to the traditional phenomenological single strand wormlike chain model with torsion in the low force/torque limit, thus suggesting that the ZZO model provides a universal microscopic model for the dsDNA. In view of the complicated nature of the double-stranded polymer and the associated interaction energies of the strands and among basepairs in the ZZO model, any analytical solution for the ZZO model would give valuable insight to the physical nature of the dsDNA. One important observation is that in the very low external force regime (< 10 pN), the DNA is basically a random coil and the elastic response is entropic in nature in which thermal effects dominate. In this case, the detail microscopic interaction at the basepair level is unimportant, as can be seen that even the simple wormlike chain model can account for the elastic behavior rather well in this regime.³ However, at somewhat larger external forces, the DNA molecule takes the *B*-form and thermal fluctuations are unimportant as compare to the external work. Motivated by this fact, hence in the force region for the transition from *B*-form to *S*-form that we are interested in, we take the classical mechanical approach to tackle the ZZO model. The shape equations governing the configuration of the dsDNA under a stretching force are derived in Sec. II. It is shown that the basic mechanism of the abrupt extension can be understood from the effective potential of the folding angle and the barrier in the potential vanishes at sufficiently large

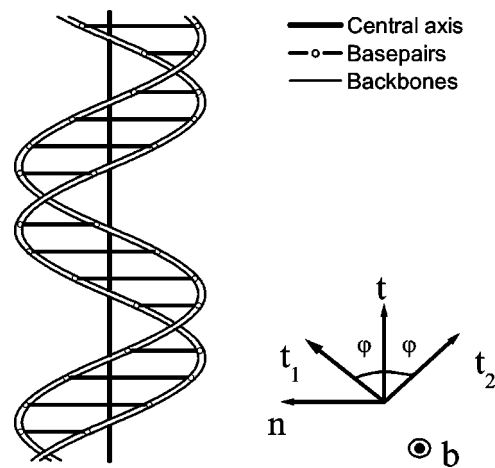


FIG. 2. Schematic representation of a double-stranded DNA molecule of the ZZO model. The right part demonstrates the definition of φ on the local $\mathbf{t}-\mathbf{n}$ plane, where \mathbf{t} , \mathbf{t}_1 , and \mathbf{t}_2 are, respectively, the tangential vectors of the central axis and the two backbones; $\mathbf{r}_2 - \mathbf{r}_1 = 2R\mathbf{b}$; φ is the folding angle. The unit vector $\mathbf{n} = \mathbf{b} \times \mathbf{t}$ is perpendicular to the $\mathbf{t}-\mathbf{b}$ plane.

forces resulting a first-order transition. The detail loci of the two backbone strands are calculated. The relative extension as a function of the stretching force is compared with the experimental data. The torque released as the dsDNA unwinds upon stretching is also calculated.

II. ZZO MODEL WITH BENDING AND BASEPAIR INTERACTION

In the ZZO model, the backbones are regarded as two inextensible wormlike chains each characterized by a (phenomenological) bending rigidity κ .^{17,18} The energy of a dsDNA is (with notation $\dot{x} \equiv dx/ds$),^{17,18}

$$E_{BS} = \int_0^L \left[\frac{1}{2} \kappa \dot{\mathbf{t}}_1^2 + \frac{1}{2} \kappa \dot{\mathbf{t}}_2^2 + \rho(\varphi) \right] ds$$

$$= \int_0^L \left[\kappa \dot{\mathbf{t}}^2 + \kappa \dot{\varphi}^2 + V(\varphi) \right] ds, \quad (1)$$

$$V(\varphi) = \frac{\kappa \sin^4 \varphi}{R^2} + \rho(\varphi),$$

where \mathbf{t} , \mathbf{t}_1 , and \mathbf{t}_2 are the tangential vectors of the central axis and two backbones, respectively, s is the arclength of the backbone, L is the total contour length of the backbone, R is the half-length of the lateral distance between two backbones. In the model each basepair is regarded as a rigid rod so R is a constant and relative sliding of the two backbones is not considered, i.e., the basepair rod is thought to be perpendicular to both backbones.³⁰ φ is called the folding angle and is equal to the half of the rotational angle from \mathbf{t}_1 to \mathbf{t}_2 (see Fig. 2). φ can vary in the range $(-\pi/2, +\pi/2)$, with $\varphi > 0$ corresponding to right-handed rotations and hence right-handed double-helical configurations and $\varphi < 0$ corresponding to left-handed ones. Note that in this model $\frac{1}{2}(\mathbf{t}_1 + \mathbf{t}_2) \neq \mathbf{t}$. Instead,

$$\dot{\mathbf{r}} = \frac{1}{2}(\dot{\mathbf{t}}_1 + \dot{\mathbf{t}}_2) = \dot{\mathbf{t}} \cos \varphi, \quad (2)$$

where $\mathbf{r} = \frac{1}{2}(\mathbf{r}_1 + \mathbf{r}_2)$ is the position vector of the central axis. Equation (2) indicates that $\cos\varphi$ measures the extent to which the backbones are “folded” with respect to the central axis. In the model, $R = 10.5 \cdot 0.34 \text{ nm} \cdot \langle \tan\varphi \rangle_{f=0} / (2\pi)$, where $\langle \rangle_{f=0}$ denotes the average under no external force.

The asymmetric base-stacking interactions $\rho(\varphi)$ originate from the weak van der Waals attraction between the polar groups in adjacent nucleotide basepairs and are usually described by the Lennard-Jones form,^{1,17,18}

$$\rho(\varphi) = \begin{cases} \frac{\epsilon}{r_0} \left[\left(\frac{c_0}{\cos\varphi} \right)^{12} - 2 \left(\frac{c_0}{\cos\varphi} \right)^6 \right] & (\varphi > 0), \\ \frac{\epsilon}{r_0} (c_0^{12} - 2c_0^6) & (\varphi \leq 0), \end{cases} \quad (3)$$

where $r_0 = 0.34 / \langle \cos\varphi \rangle_{f=0} \text{ nm}$ is the backbone arclength between adjacent bases, c_0 is a parameter related to the equilibrium distance between a DNA dimer. ϵ is the base-stacking intensity which is generally base-sequence specific.¹ As an approximation, ϵ can be taken as a constant ($= 14.0 k_B T$) from the average value of quantum-mechanically calculations on all the different DNA dimers.¹ The asymmetric base-stacking potential Eq. (3) ensures a relaxed DNA to take on a right-handed double-helix configuration (i.e., the *B*-form) with its folding angle $\cos\varphi \sim c_0$ at low temperatures. Express all lengths in units of R , i.e., $\tilde{s} \equiv s/R$ and $\tilde{L} \equiv L/R$, the energy in Eq. (1) can be scaled to the dimensionless form

$$\tilde{E}_{BS} \equiv E_{BS} R / \kappa = \int_0^{\tilde{L}} [\dot{\mathbf{t}}^2 + \dot{\varphi}^2 + \tilde{V}(\varphi)] d\tilde{s}, \quad (4)$$

where

$$\tilde{V}(\varphi) \equiv \sin^4\varphi + \tilde{\rho}(\varphi), \quad (5)$$

and

$$\tilde{\rho}(\varphi) = \begin{cases} \gamma \left[\left(\frac{c_0}{\cos\varphi} \right)^{12} - 2 \left(\frac{c_0}{\cos\varphi} \right)^6 \right] & (\varphi > 0), \\ \gamma (c_0^{12} - 2c_0^6) & (\varphi \leq 0), \end{cases} \quad (6)$$

with $\gamma \equiv \epsilon R^2 / (\kappa r_0)$. With the understanding that all quantities are properly scaled to the dimensionless quantities, the \sim can be dropped from now on unless otherwise stated. With the unit vector $\mathbf{t} \equiv (\sin\theta\cos\phi, \sin\theta\sin\phi, \cos\theta)$ as in the spherical coordinate system and for a force $\mathbf{f} = f\hat{\mathbf{z}}$ acting in the z -direction, the energy in the ZZO model can be written as

$$E_{BS} = \int_0^L (\dot{\theta}^2 + \sin^2\theta\dot{\phi}^2 + \dot{\varphi}^2 + V(\varphi) - 2\beta\cos\varphi\cos\theta) ds, \quad (7)$$

where $\beta \equiv fR^2/2\kappa$ is the dimensionless force. Minimizing E_{BS} leads to the Euler–Lagrange equations,

$$\ddot{\theta} - \sin\theta\cos\theta\dot{\phi}^2 - \beta\cos\varphi\sin\theta = 0, \quad (8)$$

$$\sin^2\theta\dot{\phi} = \text{constant}, \quad (9)$$

$$\ddot{\varphi} - \frac{V'(\varphi)}{2} - \beta\sin\varphi\cos\theta = 0, \quad (10)$$

and the boundary conditions (BCs) at the chain ends,

$$\theta(0) = \theta_o, \quad \phi(0) = \phi_o, \quad \varphi(0) = \varphi_o, \quad (11)$$

$$\dot{\theta}(L) = \dot{\phi}(L) = \dot{\varphi}(L) = 0. \quad (12)$$

The BC of $\dot{\phi}(L) = 0$ implies the constant = 0 and hence $\phi(s) = \phi_o$, i.e., the locus of the central axis lies within a plane. Thus Eq. (8) reduces to

$$\ddot{\theta} - \beta\cos\varphi\sin\theta = 0. \quad (13)$$

From the solution of $\mathbf{t}(s)$ and $\varphi(s)$, the loci of the two strands of the DNA can be obtained from

$$\mathbf{r}_{1,2}(s) = \int_0^s \mathbf{t}(s') \cos\varphi(s') ds' \pm \mathbf{b}(s), \quad (14)$$

where the unit vector $\mathbf{b}(-\mathbf{b})$ connects the central axis to the first (second) strand, with $\mathbf{r}(0) = 0$ taken as the origin. \mathbf{b} satisfies the 3×3 system of first order linear differential equations

$$\dot{\mathbf{b}} = \sin\varphi \mathbf{t} \times \mathbf{b} \quad (15)$$

with the initial condition $\mathbf{b}(0) = \mathbf{b}_o$. The differential equations can be written in matrix form as

$$\frac{d\mathbf{b}}{ds} = \sin\varphi(s) \mathbf{A}(s) \mathbf{b}, \quad (16)$$

where

$$\mathbf{A} = \begin{pmatrix} 0 & -\cos\theta & \sin\theta\sin\phi \\ \cos\theta & 0 & -\sin\theta\cos\phi \\ -\sin\theta\sin\phi & \sin\theta\cos\phi & 0 \end{pmatrix}. \quad (17)$$

The eigenvalues of \mathbf{A} are 0, $\pm i$ and are independent of s , but the corresponding eigenvectors \mathbf{t} , $\hat{\alpha}$ and $\hat{\alpha}^*$ in general depend on s .

For convenience, we shall denote the average of a quantity over the strand by

$$\overline{\dots} \equiv \frac{1}{L} \int_0^L \dots ds. \quad (18)$$

The twist *Tw* which describes the integrated rotation of the backbone around the central axis in this model is given by^{17,18}

$$\text{Tw} = \frac{1}{2\pi} \int_0^L \sin\varphi ds = \frac{L}{2\pi} \overline{\sin\varphi}. \quad (19)$$

The writhe of the central axis can also be calculated as¹⁸

$$\begin{aligned} \text{Wr} &= \frac{1}{2\pi} \int_0^L \frac{(\hat{\mathbf{z}} \times \mathbf{t}) \cdot \frac{d}{ds}(\hat{\mathbf{z}} + \mathbf{t})}{1 + \hat{\mathbf{z}} \cdot \mathbf{t}} ds \\ &= \frac{1}{2\pi} \int_0^L \frac{\sin^2\theta\dot{\phi}}{1 + \cos\theta} ds = \frac{1}{2\pi} \int_0^L (1 - \cos\theta)\dot{\phi} ds, \end{aligned} \quad (20)$$

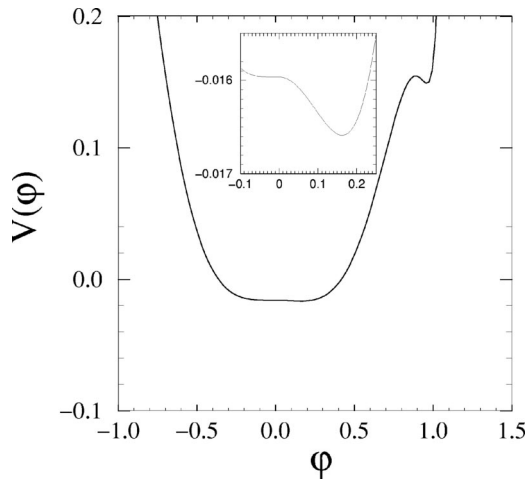


FIG. 3. $V(\varphi)$ with $c_0=0.5369$ and $\gamma=0.337$. The inset is just a blowup to show the extrema near $\varphi=0$ clearly.

when $1+\cos\theta\neq 0$. For the present case of a pure stretching force, $\dot{\phi}=0$ and so $Wr=0$. In the case of a nonzero external twisting torque,³⁷ $Wr\neq 0$ and the torque would couple with Tw and Wr via the linking number $Lk=Tw+Wr$.

The extension in the direction of the force Z is given by

$$Z = \int_0^L \cos\varphi(s) \mathbf{t} \cdot \hat{\mathbf{z}} ds = L \overline{\cos\varphi \cos\theta}. \quad (21)$$

The typical parameters (κ , c_0 and $\langle \cos\varphi \rangle_{f=0}$) in this model take the values³² $c_0 = \cos 57.53^\circ = 0.5369$, $\langle \cos\varphi \rangle_{f=0} = 0.5727$ and $\kappa/(k_B T) = 53/(2\langle \cos\varphi \rangle_{f=0})$ nm. Using these values, one has $R \approx 0.811$ nm.

III. PROPERTIES OF THE POTENTIAL $V(\varphi)$

The dimensionless potential $V(\varphi)$ depends on two dimensionless parameters c_0 and $\gamma \equiv \epsilon R^2/(\kappa r_o)$. From typical values of the various parameters,³² $c_0 \approx 0.537$, $\gamma \approx 0.337$, $V(\varphi)$ has 5 extrema for φ in the $(-\pi/2, \pi/2)$ region at $\varphi=0$, $\varphi_1 \approx 0.16277543(9.326^\circ)$, $\varphi_x \approx 0.88948346(50.96^\circ)$, and $\varphi_2 \approx 0.9611093(55.068^\circ)$ as shown in Fig. 3. $\varphi=0$ is a special singular point with $V''(0^+) < 0$ and $V''(0^-) = 0$, φ_x is a local maximum while φ_1 and φ_2 are minima. It will be shown later that many mechanical properties of the dsDNA are governed by the local minima in the long chain limit. The first derivative of V can be easily calculated and is a continuous function in φ in the entire domain,

$$V'(\varphi) = 4 \sin^3 \varphi \cos \varphi + 12 \gamma \tan \varphi \left(\frac{c_0}{\cos \varphi} \right)^6 \left(\left(\frac{c_0}{\cos \varphi} \right)^6 - 1 \right) \quad (22)$$

for $\varphi \geq 0$,

while the second term vanishes for $\varphi < 0$.

The minimum at φ_1 is very shallow from the extremum at 0 with $V(0) - V(\varphi_1) \sim 6 \times 10^{-4}$ while the barrier from the maximum at φ_x is high with $V(\varphi_x) - V(\varphi_1) \sim 0.17$. Thus in practice, very small energy fluctuations, such as thermal effects or external work will cause the state at φ_1 to be practically indistinguishable from the state at $\varphi=0$. Nevertheless, in the case of the present classical mechanical approach with

no fluctuation, φ_1 is a legitimate minimum. For the minimum at φ_2 , there is an infinite barrier for $\varphi > \varphi_2$ and the barrier from the φ_x peak is $\Delta V_2 \equiv V(\varphi_x) - V(\varphi_2) \sim 6 \times 10^{-3}$. Upon the action of an external work, such as stretching, the barrier ΔV_2 can be lower and will cause a transition to unfold the state ($\varphi \sim 0$) at a sufficiently large external work. More explicit details of this phenomenon will be given in the Sec. IV.

First consider the zero external force case, Eq. (13) becomes $\ddot{\theta}=0$ with the solution $\theta(s) = \theta_o$ under the BCs. Hence the locus of the central axis of the dsDNA is a straight line with the direction determined by the initial direction of the grafting point at $s=0$. The only equation needs to be solved from Eq. (10) is

$$2\ddot{\varphi} = V'(\varphi). \quad (23)$$

We can find immediately that $\varphi=0$, φ_1 , φ_x , and φ_2 are solutions of Eq. (23). The special case of $\varphi=0$ will be discussed in the next section. $\varphi = \varphi_x$ is out of interesting since it corresponds to the unstable state. $\varphi = \varphi_1$ and φ_2 are of special significance because they provide the asymptotic values of the solution of Eq. (23) as we can see in the following. Also notice that $\varphi = \varphi_2$ corresponds to the B -form of dsDNA. The general solution of Eq. (23) is

$$s = \pm \int_{\varphi_o}^{\varphi} \frac{du}{\sqrt{V(u) - V(\varphi_L)}}, \quad (24)$$

with $\varphi_L \equiv \varphi(L)$ to be solved from the improper integral,

$$L = \pm \int_{\varphi_o}^{\varphi_L} \frac{du}{\sqrt{V(u) - V(\varphi_L)}}. \quad (25)$$

From the behavior of $V(\varphi)$ (see Fig. 3), one can deduce the physical range of φ_L depends on the four initial range of values of φ_o , as follows: (i) $V' \leq 0$ for φ_o in $(-\pi/2, \varphi_1)$, hence Eqs. (24) and (25) take the + sign and φ_L must lie inside (φ_o, φ_1) . (ii) For φ_o in (φ_1, φ_x) ($V' \geq 0$), Eqs. (24) and (25) take the - sign and φ_L in (φ_1, φ_o) . (iii) For φ_o in (φ_x, φ_2) ($V' \leq 0$), Eqs. (24) and (25) take the + sign and φ_L in (φ_o, φ_2) . (iv) For φ_o in $(\varphi_2, \pi/2)$ ($V' \geq 0$), Eqs. (24) and (25) take the - sign and φ_L in (φ_2, φ_o) . In practical situations, the folding angle at the initial grafting point is usually not subjected to extra folding or unfolding from its natural state, therefore in most experimental cases, φ_o is not far from φ_2 and lies in regions (iii) or (iv). Thus in what follows, we shall consider mostly the case of φ_o in regions (iii) or (iv), but similar analysis will hold for the other two regions. Before we proceed to evaluate the improper integral in Eq. (25), we shall estimate the order of magnitude of the dimensionless (in unit of R) DNA backbone length L . One easily finds, under usual experimental situations, $L \approx 50$ (DNA length/ ℓ_p), where ℓ_p is the persistent length of the DNA. Therefore in most experimental situations, $L \gg 1$ and the $L \rightarrow \infty$ limit is of practical significance. To find φ_L in the large L limit, consider the following improper integral:

$$\int_{\varphi_o}^{\varphi_2 - \delta} \frac{du}{\sqrt{V(u) - V(\varphi_2 - \delta)}}, \quad (26)$$

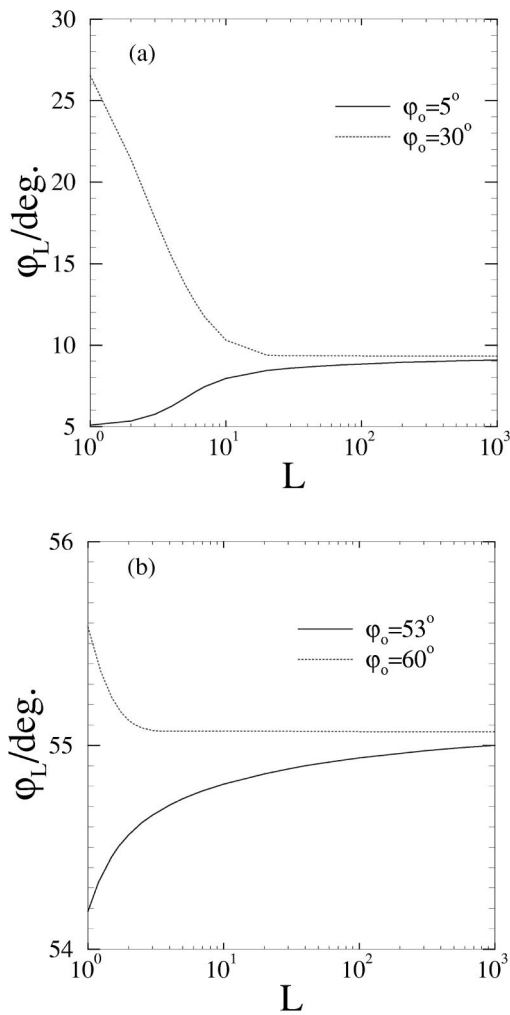


FIG. 4. φ_L solved from Eq. (25) as a function of L for the zero force case with various initial values of φ_o . (a) φ_o in regions (i) and (ii), $\varphi_L \rightarrow \varphi_1 \approx 9.326^\circ$. (b) φ_o in regions (iii) and (iv), $\varphi_L \rightarrow \varphi_2 \approx 55.068^\circ$.

where $\delta > 0$ is a small quantity. For φ_o in region (iii), the dominant part of the above integral can be obtained by a systematic expansion as

$$2 \sqrt{\frac{\varphi_2 - \varphi_o - \delta}{-V'(\varphi_2 - \delta)}} \left[1 - \frac{V''(\varphi_2 - \delta)}{12V'(\varphi_2 - \delta)} (\varphi_2 - \varphi_o - \delta) + \dots \right]$$

$$= 2 \sqrt{\frac{\varphi_2 - \varphi_o}{\delta V''(\varphi_2)}} \left[1 + \frac{\varphi_2 - \varphi_o}{12\delta} + \dots \right].$$

This integral diverges as $\delta \rightarrow 0$ and hence it follows that as $L \rightarrow \infty$, $\varphi_L \rightarrow \varphi_2^-$. Similarly, for φ_o in regions (iv), (i), and (ii), φ_L approaches φ_2^+ , φ_1^- , φ_1^+ , respectively, as $L \rightarrow \infty$. For general given values of L , φ_L is solved numerically from the nonlinear equation (25). Figure 4 displays the variation of φ_L as a function of L for various initial values of φ_o . As shown, φ_L indeed approaches the constant value of $\varphi_2(\varphi_1)$ as L becomes large in regions (iii) and (iv) [(i) and (ii)]. Figure 5(a) shows $\varphi(s)$ for finite L and Figs. 5(b) and 5(c) display $\varphi(s)$ with $L \rightarrow \infty$ for various initial values of φ_o that correspond to the four regions. In practice, $\varphi_o \sim \varphi_2$ and thus $\varphi_L \approx \varphi_2$ for $L \gg 1$. Therefore, from the equation of motion $\dot{\varphi}^2 = V(\varphi) - V(\varphi_2)$, φ must be confined in the allowed re-

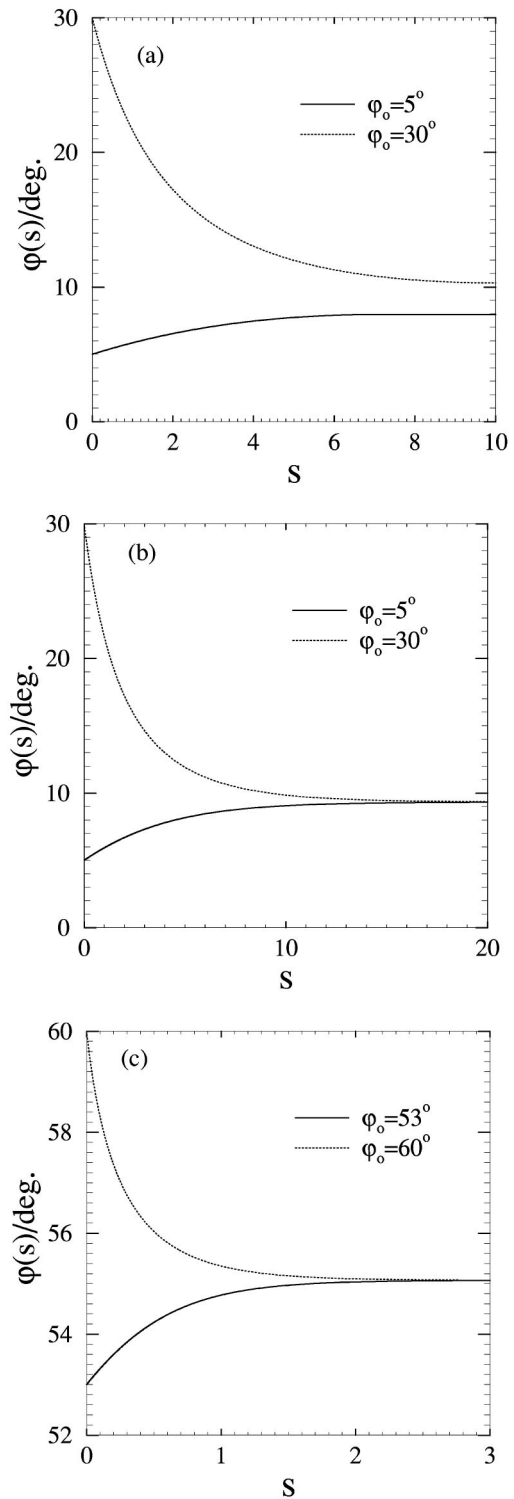


FIG. 5. $\varphi(s)$ for various initial values of φ_o . (a) for $L=10$ and (b) $L \rightarrow \infty$ (c) also for $L \rightarrow \infty$ but for $\varphi_o = 53^\circ$ and 60° .

gime with $V(\varphi) \geq V(\varphi_2)$, as depicted in Fig. 6. In most experimental situations at room temperatures, since $k_B TR/\kappa \sim 0.018$ which is appreciably less than $L\Delta V_2$ (since $L \gg 100$ in experiments), the DNA will remain in the state φ_2 if it is initial near this state. This again justifies our classical mechanic approach of neglecting thermal fluctuations in this region.

Loci of the two strands: Since for $\beta=0$, $\mathbf{t}(s) = \mathbf{t}_o$

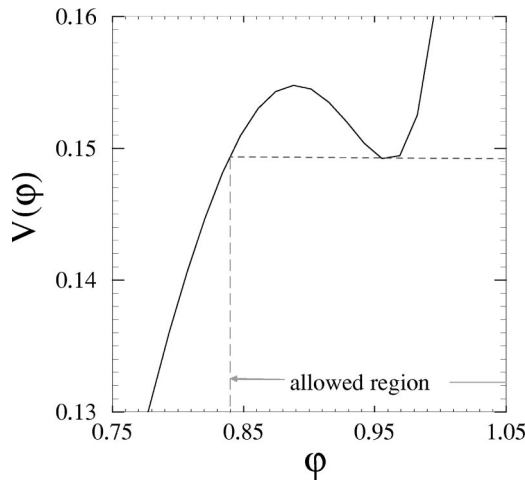


FIG. 6. Close up of $V(\varphi)$ near the minimum at φ_2 showing the allowed region for φ in the $L \rightarrow \infty$ limit. The dotted horizontal line indicates the value of $V(\varphi_L) \approx V(\varphi_2)$.

$\equiv (\sin \theta_o \cos \phi_o, \sin \theta_o \sin \phi_o, \cos \theta_o)$ is a constant, the matrix \mathbf{A} is also a constant with eigenvalues $0, i$ and $-i$ and the corresponding normalized eigenvectors are $\mathbf{t}_o, \hat{\alpha},$ and $\hat{\alpha}^*$, respectively. Defining $\xi(s) \equiv \int_0^s ds' \sin \varphi(s')$ and write

$$\hat{\alpha} = (\alpha_x e^{i\eta_x}, \alpha_y e^{i\eta_y}, \alpha_z e^{i\eta_z}), \quad (27)$$

where $\alpha_x^2 + \alpha_y^2 + \alpha_z^2 = 1$ and the η 's are known, the general solution of \mathbf{b} is given by

$$\mathbf{b} = C\mathbf{t}_o + B(\alpha_x \cos[\xi(s) + \eta_x + \delta], \alpha_y \cos[\xi(s) + \eta_y + \delta], \alpha_z \cos[\xi(s) + \eta_z + \delta]), \quad (28)$$

where the constants $C, B,$ and δ are to be determined from the initial condition of \mathbf{b}_o . For large L and $s \gg 1,$ $\xi(s) \approx \sin \varphi_2 s$ (or $\sin \varphi_1 s,$ depending on the value of φ_o), and \mathbf{b} rotates along the central axis with a fixed frequency of $\sin \varphi_2$. A convenient choice of \mathbf{b}_o would be $(1, 0, 0)$. For example, if $\mathbf{t}_o = (0, 0, 1)$ (i.e., $\theta_o = 0$), then $\mathbf{b}(s) = [\cos \xi(s), \sin \xi(s), 0]$. Figure 7 shows a long dsDNA in its B -form at two different initial folding angles. For low values of φ_o , the double helix has a large pitch, the realistic case resembles the configuration depicted with a $\varphi_o \sim 53^\circ - 56^\circ$. It should be noted that in Refs. 17 and 18 only the ground state eigenvalues and eigenfunction can be calculated numerically in practice and hence only quantities average over the whole chain can be calculated. But our present classical mechanics approach can compute the detail structural configurations of the dsDNA.

IV. SOME SPECIAL CASES

A. Vanishing folding at the grafting point: $\varphi_o = 0$

This is the case that corresponds to parallel grafting the two strands, with $\mathbf{t}_1(0) = \mathbf{t}_2(0)$. In this case, the solution of φ is trivial

$$\varphi(s) = 0, \quad (29)$$

and the differential equation for θ reduces to

$$\ddot{\theta} = \beta \sin \theta, \quad \theta(0) = \theta_o, \quad \dot{\theta}(L) = 0. \quad (30)$$

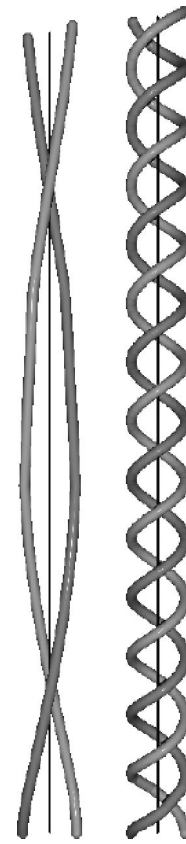


FIG. 7. Segments of double stranded DNA under no force for two different values of $\varphi_o = 30^\circ$ (left) and $\varphi_o = 53^\circ$ (right). The dark line denotes the central axis. $\theta_o = 0^\circ, L = \infty$.

As can be easily seen that the solution of θ reduces to the same solution of the wormlike chain (WLC) model of a chain of bending stiffness 2κ under a force f (Ref. 33) (see Appendix), with

$$\sqrt{2}\beta s = \int_{\theta_o}^{\theta} \frac{du}{\sqrt{\cos \theta_L - \cos u}}. \quad (31)$$

And the solution can be put in the analytic closed form³⁸ as

$$\theta(s) = 2 \cos^{-1}[k \operatorname{sn}(F(\zeta_o, k) + \beta s, k)], \quad (32)$$

where $k \equiv \cos(\theta_L/2), \sin \zeta_o = (1/k)\cos(\theta_o/2), F$ and sn are the elliptic function of the first kind and Jacobian elliptic sine function, respectively. $k \equiv \cos(\theta_L/2)$ is solved from the boundary condition at the $s = L$ end,

$$K(k) = F(\zeta_o, k) + \beta L, \quad (33)$$

where K is the complete elliptic function of the first kind.

B. $\theta_o = \varphi_o = 0$

This case corresponds to grafting both strands parallel to \mathbf{f} . One gets the trivial solution of

$$\theta(s) = 0, \quad \varphi(s) = 0, \quad (34)$$

independent of the length L .

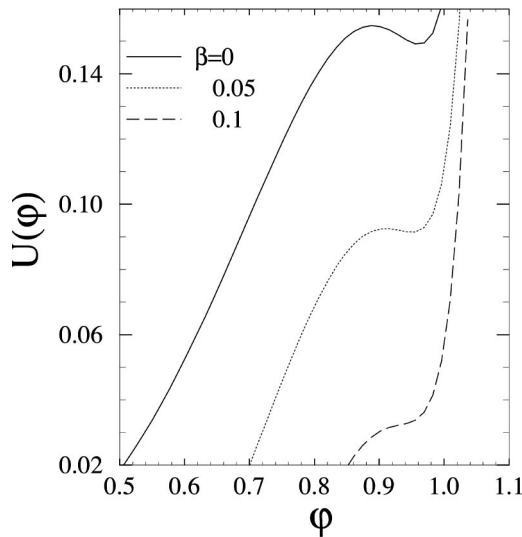


FIG. 8. $U(\varphi)$ with $c_0=0.5369$ and $\gamma=0.337$ for different values of the stretching force β .

C. t_o parallel to f : $\theta_o=0$, but $\varphi_o \neq 0$

In this case,

$$\theta(s)=0, \tag{35}$$

$$\ddot{\varphi} - \frac{1}{2}V'(\varphi) - \beta \sin \varphi = 0, \quad \varphi(0) = \varphi_o, \quad \dot{\varphi}(L) = 0. \tag{36}$$

Defining the effective potential of the DNA under a stretching force as

$$U(\varphi) \equiv V(\varphi) - 2\beta \cos \varphi, \tag{37}$$

the differential equation in φ can be solved in a similar way as in the $f=0$ case (see Sec. IV) with U replacing V , by evaluating the integral

$$s = \pm \int_{\varphi_o}^{\varphi} \frac{du}{\sqrt{U(u) - U(\varphi_L)}}, \tag{38}$$

and $\varphi_L \equiv \varphi(L)$ is obtained by solving it from the improper integral,

$$L = \pm \int_{\varphi_o}^{\varphi_L} \frac{du}{\sqrt{U(u) - U(\varphi_L)}}. \tag{39}$$

Or $\varphi(s)$ can also be numerically solved directly from the second-order o.d.e., by the shooting method to match the BCs at L .

Much insight about the stretching transition of the DNA from the B -form to the S -form can be gained by considering the properties of the effective potential $U(\varphi)$ as β increases. Figure 8 displays $U(\varphi)$ for various stretching forces. It can be easily seen that $\varphi=0$ is always an extremum for U . For very low values of β , U still has two minima near φ_1, φ_2 and one maximum near φ_x with their values being dependent on β . As β increases, the value of φ_1 decreases and at $\beta \approx 0.0475$, φ_1 coincides with the extremum at 0 and the extremum at $\varphi=0$ becomes a minimum. At the same time, φ_2 decreases and φ_x increases as β increases and eventually

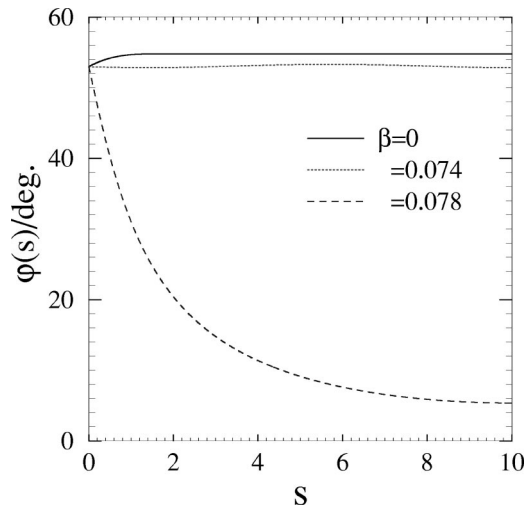


FIG. 9. $\varphi(s)$ for different stretching forces β for $\theta_o=0^\circ$ and $\varphi_o=53^\circ$. $L=10$.

these two extrema annihilate at φ_t when $\beta = \beta_t$ where β_t and φ_t can be obtained from the conditions $U''(\varphi_t) = U'(\varphi_t) = 0$. One easily finds the threshold dimensionless force to be $\beta_t = 0.076352$ and $\varphi_t = 0.932461$. For $\beta > \beta_t$, $U(\varphi)$ has only one minimum at $\varphi=0$, the unfold state. The transition from the folded state to the unfold state occurs at β_t for this $\theta_o=0$ case, which corresponds to $f \sim 45$ pN which is not far from the threshold of ~ 65 pN as observed in force experiments (in which θ_o is not known). Furthermore, because our approach ignores thermal fluctuation effects which may still has some contributions to the elasticity near the onset of transition in real experiments, indeed the threshold force calculated in our approach is slightly less than in experiments as expected. Figure 9 shows the solution of $\varphi(s)$ for forces below and above the transition for a DNA of $L=10$ with $\theta_o=0$. For $\beta < \beta_t$ the whole DNA is still folded with $\varphi(s) \approx \varphi_o$, but for $\beta > \beta_t$, $\varphi(s)$ rapidly decreases with s indicating the DNA gets unfolded by the external force and the degree of unfolding is more near the DNA end where the external force is applied.

V. UNDER A STRETCHING FORCE ($\beta > 0$)

A. Small force

Before we proceed with the numerical solution, one can estimate the order of magnitude of the dimensionless force β in most current experimental situations. For nowadays experiments using micromechanics and optical/magnetic tweezers working with DNA, f is around the pN range, with $f/\text{pN} \sim 0.1$ to 100. And with the typical values of R and κ , one has $\beta \approx 1.8 \times 10^{-3} (f/\text{pN})$. Thus in most experimental conditions, $\beta \sim 0.001$ to 0.1, i.e., $\beta \ll 1$ is quite well satisfied in most cases. Therefore, it makes sense to consider perturbation around the $\beta=0$ solution. For small β , one expects $\theta(s) = \theta_o - \beta \Theta(s)$ and $\varphi(s) = \varphi^{(o)}(s) - \beta \Phi(s)$, where $\varphi^{(o)}(s)$ satisfies Eq. (23). Substituting to Eqs. (10) and (13), one gets

$$\ddot{\Theta} - \beta \Theta \cos \varphi^{(o)} \cos \theta_o + \cos \varphi^{(o)} \sin \theta_o = 0, \tag{40}$$

$$\ddot{\Phi} - \frac{\Phi}{2} V''(\varphi^{(o)}) + \sin \varphi^{(o)} \cos \theta_o = 0, \quad (41)$$

with the boundary conditions $\Theta(0) = \Theta'(L) = \Phi(0) = \Phi'(L) = 0$. The equations become decoupled and each can be solved more easily. However, the main purpose here is not to obtain the numerical solutions for $\Phi(s)$ and $\Theta(s)$, rather the behavior of $\Phi(s)$ can give some insight on the linear extension coefficient of the dsDNA. Unlike the inextensible WLC model, the dsDNA in ZZO model can be extended by unfolding the folding angle φ upon a stretching force. In the simplest case of stretching the DNA along the initial grafting direction, i.e., $\theta_o = 0$, the extension along the force direction relative to the zero force case is (here L is the contour length and the dimensionless contour is written explicitly as L/R)

$$\frac{Z}{L} - \left(\frac{Z}{L} \right)_{f=0} = \beta \overline{\Phi \sin \varphi^{(o)}}. \quad (42)$$

Hence the linear extension coefficient [1/(force constant)] is

$$\frac{1}{\text{force constant}} = \frac{R^2 L}{2\kappa} \overline{\Phi \sin \varphi^{(o)}} \sim \frac{R^2 L}{2\kappa} \quad \text{for } \theta_o = 0, \quad (43)$$

where $\overline{\Phi \sin \varphi^{(o)}}$ is the integral average in the region of $[0, L]$. The leading scaling behavior can be estimated in the $L \gg 1$ case, since $\overline{\Phi \sin \varphi^{(o)}} \sim 2 \sin^2 \varphi_2 \cos \theta_o / V''(\varphi_2)$ for φ_o in regions (iii) and (iv) [for regions (i) and (ii), $\varphi_2 \rightarrow \varphi_1$]. Although $V''(\varphi_2)$ and φ_2 has some dependence on R^2/κ through γ [see Eq. (5)], the dependence on L and κ is much weaker than the $R^2 L / (2\kappa)$ factor. Thus one has the leading scaling behavior in Eq. (43).

B. Solution of $\theta(s)$ and $\varphi(s)$

For given values of β and L and general initial values θ_o and φ_o , $\theta(s)$ and $\varphi(s)$ are solved numerically using the finite difference plus the shooting method. For given θ_o and φ_o , one varies $\dot{\theta}(0)$ and $\dot{\varphi}(0)$ until the boundary conditions $\dot{\theta}(L) = \dot{\varphi}(L) = 0$ are satisfied. Extra caution has to be taken especially in the large L case since one can run into numerical instability. Figure 10 shows the solutions of $\theta(s)$ and $\varphi(s)$ for given L and φ_o for various values of β . Again the DNA remains highly folded with $\varphi(s) \approx \varphi_o$ for forces below the transition, but becomes unfolded rapidly along the DNA chain from the initial end for stretching forces greater than the threshold. The bending angle $\theta(s)$ all decreases from the initial end for nonzero external force showing the DNA is aligned by the force. Larger decrease in the $\theta(s)$ curve occurs as the external force increases across the transition indicating that the DNA is relatively easier to bend in the S -form. Figure 11 shows the configurations of the dsDNA under two different stretching forces below and above the threshold value. The dsDNA gets untwisted considerably by the pure stretching force above the threshold. Such untwisting will give rise to a torque and cause the DNA to rotate about its central axis.

Figure 12 shows the twist of the DNA as calculated in Eq. (19) with $\theta_o = 10^\circ$ and $L = 10$ as a function of the stretching force. Tw decreases with increasing β as expected and a

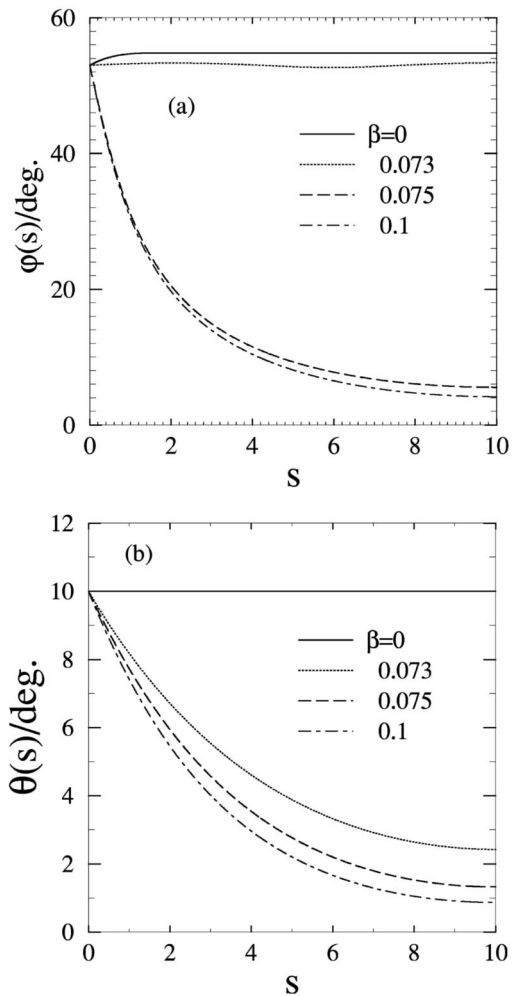


FIG. 10. (a) $\varphi(s)$ for different stretching forces β . $\theta_o = 10^\circ$, $\varphi_o = 53^\circ$, and $L = 10$. (b) $\theta(s)$ with the same parameters as in (a).

sharp drop occurs at the threshold force of about $\beta \approx 0.075$ which is not far from the threshold value ($\beta_t = 0.076352$) in the $\theta_o = 0$ case. The value of Tw decreases from about 1.3 turn to 0.4 turn and the DNA unwinds with a rotation of about 320° (for $L = 10$). Thus the dsDNA undergoes a self untwist of about $\Delta \text{Tw} / L \sim -0.09$ across the transition from its B -form to S -form. The mean angle from the force direction $\bar{\theta}$ as a function of β is shown in Fig. 13. $\bar{\theta}$ decreases with increasing stretching force indicating that the DNA is more aligned by a stronger force. However the drop in $\bar{\theta}$ is less prominent near the transition.

C. Relative extension

The most common quantity measured in force experiments is the relative extension of the DNA, defined as Z/L_o , where Z is the end-to-end distance along the direction of the force and L_o is the contour length of the B -form under no force. In the present model L_o is just the contour length of the central axis, with $L_o = (\int_0^L \cos \varphi(s) ds)_{f=0}$. The relative extension is given by

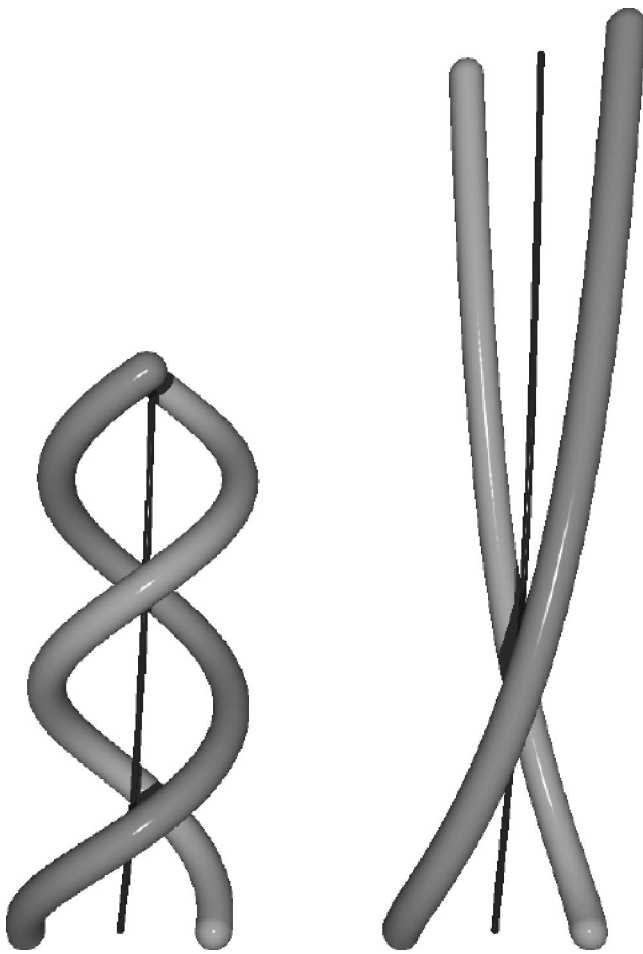


FIG. 11. DNA double helix under a reduced stretching force of $\beta=0.073$ (left) and $\beta=0.075$ (right). $(\theta_o, \varphi_o) = (10^\circ, 53^\circ)$. $L=10$.

$$\frac{Z}{L_o} = \frac{\overline{\cos \varphi \cos \theta}}{\overline{\cos \varphi}|_{f=0}} \quad (44)$$

which in general is dependent on the initial values of (φ_o, θ_o) and the length L . Figure 14 shows the relative ex-

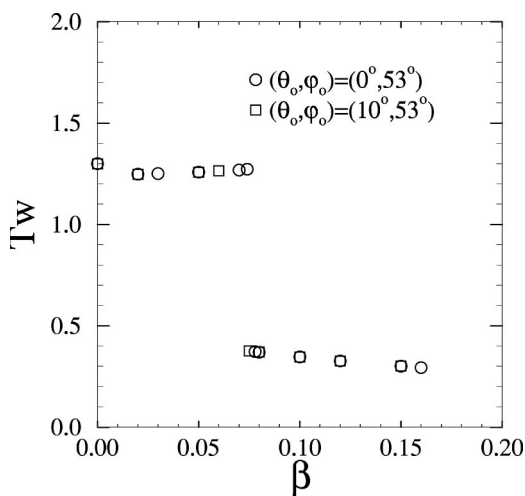


FIG. 12. The twist of the DNA as a function of β for different values of (θ_o, φ_o) . $L=10$.

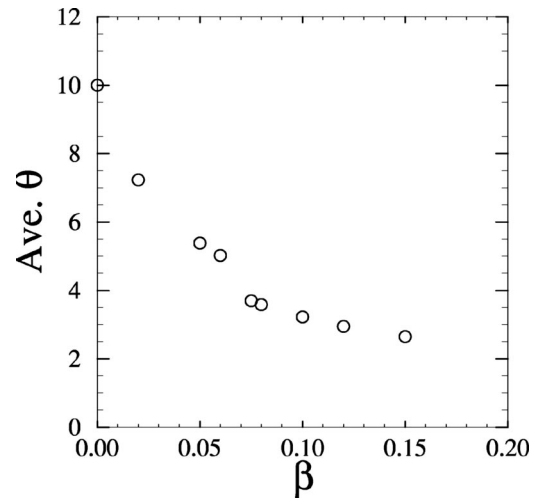


FIG. 13. Average angle, $\bar{\theta}$, from the force direction as a function of β for different values of $(\theta_o, \varphi_o) = (10^\circ, 53^\circ)$ and $L=10$.

tension versus the scaled force β for $L=10$. The experimental data is also shown in the inset for comparison. Our results show an increase of about 1.65 times in the relative extension across the transition and appears to be not sensitive to the initial values of (φ_o, θ_o) . In the limit of $L \rightarrow \infty$, $\overline{\cos \varphi}|_{f=0} \rightarrow \cos \varphi_2(\cos \varphi_1)$ if φ_o lies in regions (iii) and (iv) [(i) and (ii)]. In the strong force limit $\cos \varphi \cos \theta \rightarrow 1$, then $Z/L_o \approx 1/\cos \varphi_2 \approx 1.7$ which is good agreement with experimental results of about 1.65. The slightly larger value in our prediction is due to the fact that the (weak) thermal entropic effects ignored in our approach would cause the DNA to be less extensible.

D. Self-unwinding and torque associated with the $B \rightarrow S$ transition

As the dsDNA is stretched from the B -form to S -form, it also undergoes a self-untwisting and the amount of untwisting can be estimated in the large L limit using Eq. (19) to give

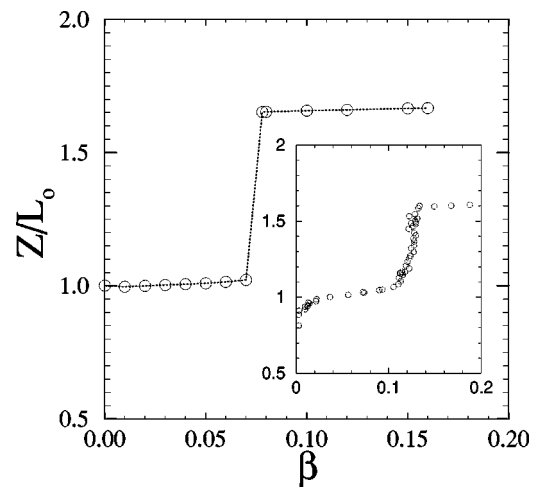


FIG. 14. Relative extension as a function of β for $(\theta_o, \varphi_o) = (0^\circ, 53^\circ)$ and $L=10$. The inset is a replot of Fig. 1 using the dimensionless force β .

$$\Delta Tw/L \sim -\sin \varphi_t / (2\pi) \sim -0.13, \quad (45)$$

which corresponds to $\Delta Tw/L_o \sim -0.13/\cos \varphi_2 \sim -80^\circ$, or translate back to $\sim 100^\circ$ per nm of central DNA axis length, i.e., it amounts to a self-untwisting of $\sim 34^\circ/\text{bp}$, which indicates that the dsDNA is almost fully untwisted acrossing the $B \rightarrow S$ transition (1 rev./10.5 bp = $34.3^\circ/\text{bp}$). Current fluorescence experimental techniques can measure this untwisting.

The amount of work, or torque released across the $B \rightarrow S$ transition upon stretching the dsDNA can also be estimated in our approach. The change in energy associated with the transition can be calculated as follows: With our loss of generality, we take the $\theta_o = 0$ as the initial grafted condition, then from Eqs. (36) and (37) with the effective potential $U(\varphi)$, one has

$$E = \int_0^L [\dot{\varphi}^2 + U(\varphi)] ds. \quad (46)$$

Thus the minimized energy, E_{\min} is given by

$$\frac{E_{\min}}{L} = \frac{2}{L} \int_0^L U(\varphi) ds - U(\varphi_L). \quad (47)$$

In the $L \gg 1$ case near $\beta = \beta_t$, $\varphi_L \approx \varphi_t$ in the B state while $\varphi_L \sim 0$ in the S state. Thus the decrease in energy across the $B \rightarrow S$ transition is

$$\frac{\Delta E}{L} \approx U(\varphi_t) - U(0) = V(\varphi_t) + 2\beta_t(1 - \cos \varphi_t). \quad (48)$$

Plug in the values of β_t and φ_t , one gets $\Delta E/L \approx 0.2117$. The mean torque $\bar{\Gamma}$ is given by the ratio of ΔE to the amount untwisted. Using the above result for the self untwist in Eq. (45) and expressing the final result back to dimensional units, one finally gets

$$\bar{\Gamma} = \frac{\kappa}{R} \csc \varphi_t (V(\varphi_t) + 2\beta_t(1 - \cos \varphi_t)). \quad (49)$$

Using typical values of the parameters of $R \approx 0.811$ nm and κ , one has $\bar{\Gamma} \sim 60$ pN nm. This value is consistent with the recent fluorescence experiment of DNA rotating during transcription by RNA polymerase,³⁴ which reported a lower limit of the mean torque of ~ 5 pN nm as the DNA rotates.

VI. DISCUSSIONS AND OUTLOOK

In this paper, we obtained the detail structural information on the transition from the B -form to the S -form dsDNA using the classical mechanics approach. Our approach works rather well due to the fact that thermal fluctuations is relatively weak when the DNA is in its B -form: it is already quite straight and hence entropic effects can be safely ignored. Differential equations governing the shape of the dsDNA can be derived and in some situations allow for some valuable analytical results. The loci of the dsDNA can be explicitly calculated. The extension-force results agree rather well with experimental data, with an excellent agreement of 1.7 times of increase of extension in the transition of the B -form to the S -form. It is worth to note that molecular mechanics simulations of a dsDNA under stress^{6,35} also re-

vealed that the double helix unwinds upon stretching if both 3' ends are being pulled, and a plateau in the force-extension curve qualitatively similar to Fig. 14 is also obtained. In our calculations, the threshold force for the onset of transition is predicted to be about 45 pN which is about 20% less than as observed in experiments, and this discrepancy is believed to be mainly due to the neglect of entropic elasticity and the unknown grafting condition of the initial end (θ_o and φ_o) in experiments. The most valuable information in the present study is to show that the sharp rise in extension is a first-order transition. The nature of this transition can be summarized by the effective potential as shown in Fig. 8 (even though it is for the case of $\theta_o = 0$). The physical picture is that of the energy barrier being removed as the external stretching is beyond the threshold force, which results in a first-order phase transition. The basic mechanism is similar to the first-order transition in unwinding a collapse homopolymer in a poor solvent by an external force.³⁶ We anticipate that for the realistic case of a DNA which is a heteropolymer and the attractive interactions may vary in strength for different basepairs, the sharp first-order nature of the transition would remain to be true. The key point is due to the short-range nature of the attractive interactions for adjacent basepair planes along the DNA. As the tension along the DNA is increased by the stretching force, the attractions are overcome for sufficiently large forces and the separation between the basepair planes is increased. Since the basepair plane attractions are all short-ranged, once the separation is beyond the range of attraction, the restoring force disappears and the DNA will be stretched abruptly. Across the $B \rightarrow S$ transition, the dsDNA also undergoes a self-untwisting of $\sim 34^\circ$ per bp which indicates an almost complete unwinding of the original B -DNA. This large untwisting would give rise to a torque that can be used in DNA motor design and the $B \rightarrow S$ transition thus provides a switch for such a motor. This large untwisting would couple strongly to an external torque applied to the DNA end³⁷ and result in supercoiling/uncoiling. Current experimental techniques should be able to measure this large amount of untwisting. Our classical mechanical approach can include the effect of applying an external torque and differential equations can also be derived. Left-handed Z -form DNA can be produced upon the action of a sufficiently negative torque. These results will be published elsewhere.³⁷ Hysteresis is expected if the stretching/releasing rate of the force is fast enough because of the first-order nature of the B to S transition. If the dsDNA is brought to the metastable state, the dynamics of the chain returning to its equilibrium configuration is expected to be hindered by the activation barrier. The corresponding dynamic responses of the dsDNA under stresses is very interesting and it will be investigated in the framework of the present model in our future studies.

ACKNOWLEDGMENTS

This work has been supported by the National Science Council of Republic of China under Grants No. NSC91-2112-M008-049 and No. NSC91-2112-M032-006.

APPENDIX: WORMLIKE CHAIN MODEL

The WLC model regards a dsDNA molecule as a slender cylindrical elastic rod with a fixed contour length L with the energy,

$$E_{WLC} = \int_0^L \left[\frac{\kappa}{2} \left(\frac{d\mathbf{t}}{ds} \right)^2 - \mathbf{f} \cdot \mathbf{t} \right] ds, \tag{A1}$$

where κ is the bending stiffness. Taking the coordinate system with $\mathbf{f} = f\hat{\mathbf{z}}$ and $\mathbf{t} = (\sin\theta\cos\phi, \sin\theta\sin\phi, \cos\theta)$, minimizing E_{WLC} for given initial $\mathbf{t}(0) = (\sin\theta_o\cos\phi_o, \sin\theta_o\sin\phi_o, \cos\theta_o)$, one arrives at the equations,

$$\ddot{\theta} - \sin\theta\cos\theta\dot{\phi}^2 - (f/\kappa)\sin\theta = 0, \tag{A2}$$

$$\sin^2\theta\dot{\phi} = \text{constant}, \tag{A3}$$

with boundary conditions $\theta(0) = \theta_o$, $\phi(0) = \phi_o$, and $\dot{\theta}(L) = \dot{\phi}(L) = 0$. The solution is easily obtained to be $\phi(s) = \phi_o$ and

$$\sqrt{\frac{2f}{\kappa}}s = \int_{\theta_o}^{\theta} \frac{du}{\sqrt{\cos\theta_L - \cos u}}, \tag{A4}$$

where $\theta_L \equiv \theta(L)$ is obtained by solving

$$\sqrt{\frac{2f}{\kappa}}L = \int_{\theta_o}^{\theta_L} \frac{du}{\sqrt{\cos\theta_L - \cos u}}. \tag{A5}$$

More details of the solution of the WLC model can be found in Ref. 33.

Defining $k \equiv \cos(\theta_L/2)$ and transforming variables with $\cos(\theta/2) = k \sin\zeta$, the exact solution can be put into the closed form,³⁸

$$\cos\frac{\theta(s)}{2} = k \operatorname{sn} \left[F(\zeta_o, k) + \sqrt{\frac{f}{\kappa}}s, k \right], \tag{A6}$$

where $\sin\zeta_o = \cos(\theta_o/2)/k$. And $k \equiv \cos(\theta_L/2)$ is solved from the boundary condition at the $s=L$ end,

$$K(k) - F(\zeta_o, k) = \sqrt{\frac{f}{\kappa}}L, \tag{A7}$$

where K is the complete elliptic function of the first kind.

¹W. Saenger, *Principles of Nucleic Acid Structure* (Springer-Verlag, New York, 1984).

²J. D. Watson, N. H. Hopkins, J. W. Roberts, J. A. Steitz, and A. M. Weiner,

Molecular Biology of the Gene, 4th ed. (Benjamin/Cummings, California, 1987).

³S. B. Smith, L. Finzi, and C. Bustamante, *Science* **258**, 1122 (1992).
⁴D. Bensimon, A. J. Simon, V. Croquette, and A. Bensimon, *Phys. Rev. Lett.* **74**, 4754 (1995).
⁵T. R. Strick, J. F. Allemand, D. Bensimon, A. Bensimon, and V. Croquette, *Science* **271**, 1835 (1996).
⁶P. Cluzel, A. Lebrun, C. Heller, R. Lavery, J. L. Viovy, D. Chatenay, and F. Caron, *Science* **271**, 792 (1996).
⁷S. B. Smith, Y. Cui, and C. Bustamante, *Science* **271**, 795 (1996).
⁸L. Stewart, M. R. Redinbo, X. Qiu, W. G. J. Hol, and J. J. Champoux, *Science* **279**, 1534 (1998).
⁹V. V. Rybenkov, C. Ullsperger, A. V. Vologodskii, and N. R. Cozzarelli, *Science* **277**, 690 (1997).
¹⁰T. R. Strick, V. Croquette, and D. Bensimon, *Proc. Natl. Acad. Sci. U.S.A.* **95**, 10579 (1998).
¹¹J. F. Allemand, D. Bensimon, R. Lavery, and V. Croquette, *Proc. Natl. Acad. Sci. U.S.A.* **95**, 14152 (1998).
¹²J. F. Léger, J. Robert, L. Bourdieu, D. Chatenay, and J. F. Marko, *Proc. Natl. Acad. Sci. U.S.A.* **95**, 12295 (1998).
¹³J. F. Léger, G. Romano, A. Sarkar, J. Robert, L. Bourdieu, D. Chatenay, and J. F. Marko, *Phys. Rev. Lett.* **83**, 1066 (1999).
¹⁴T. Nishinaka, Y. Ito, S. Yokoyama, and T. Shibata, *Proc. Natl. Acad. Sci. U.S.A.* **94**, 6623 (1997).
¹⁵T. Nishinaka, A. Shinohara, Y. Ito, S. Yokoyama, and T. Shibata, *Proc. Natl. Acad. Sci. U.S.A.* **95**, 11071 (1998).
¹⁶H. Zhou and Z.-c. Ou-Yang, *Phys. Rev. E* **58**, 4816 (1998); *J. Chem. Phys.* **110**, 1247 (1999).
¹⁷H. Zhou, Y. Zhang, and Z.-c. Ou-Yang, *Phys. Rev. Lett.* **82**, 4560 (1999).
¹⁸H. Zhou, Y. Zhang, and Z.-c. Ou-Yang, *Phys. Rev. E* **62**, 1045 (2000).
¹⁹M.-H. Hao and W. K. Olson, *Biopolymers* **28**, 873 (1989); *Macromolecules* **22**, 3292 (1989).
²⁰J. F. Marko and E. D. Siggia, *Science* **265**, 506 (1994); *Macromolecules* **28**, 8759 (1995).
²¹C. Bustamante, J. F. Marko, E. D. Siggia, and S. Smith, *Science* **265**, 1599 (1994).
²²B. Fain, J. Rudnick, and S. Östlund, *Phys. Rev. E* **55**, 7364 (1997).
²³J. D. Moroz and P. Nelson, *Proc. Natl. Acad. Sci. U.S.A.* **94**, 14418 (1997).
²⁴A. V. Vologodskii and J. F. Marko, *Biophys. J.* **73**, 123 (1997).
²⁵B.-Y. Ha and D. Thirumalai, *J. Chem. Phys.* **106**, 4243 (1997).
²⁶P. Cizeau and J.-L. Viovy, *Biopolymers* **42**, 383 (1997).
²⁷C. Bouchiat and M. Mézard, *Phys. Rev. Lett.* **80**, 1556 (1998).
²⁸P. Nelson, *Phys. Rev. Lett.* **80**, 5810 (1998).
²⁹C. Bouchiat and M. Mézard, *Eur. Phys. J. E* **2**, 377 (2000).
³⁰T. B. Liverpool, R. Golestanian, and K. Kremer, *Phys. Rev. Lett.* **80**, 405 (1998).
³¹A. Sarkar, J.-F. Léger, D. Chatenay, and J. F. Marko, *Phys. Rev. E* **63**, 051903 (2001).
³²Z. Zhou and P.-Y. Lai, *Chem. Phys. Lett.* **346**, 449 (2001).
³³P.-Y. Lai and Z. Zhou, *Chin. J. Phys. (Taipei)* **39**, 641 (2001).
³⁴Y. Harada, O. Ohara, A. Takatsuki, H. Itoh, N. Shimamoto, and K. Kinoshita, *Nature (London)* **409**, 113 (2001).
³⁵A. Lebrun and R. Lavery, *Nucleic Acids Res.* **24**, 2260 (1996).
³⁶P.-Y. Lai, *Phys. Rev. E* **53**, 3819 (1996); **58**, 6222 (1998).
³⁷P.-Y. Lai and Z. Zhou, *Chin. J. Phys. (Taipei)* **40**, 465 (2002).
³⁸P.-Y. Lai, G. Rowlands, and Z. Zhou (unpublished).